RASĀYAN *J. Chem.*
Vol. 17 | No. 4 |1426-1435| October - December | 2024
ISSN: 0974-1496 | e-ISSN: 0976-0083 | CODEN: RJCABP
http://www.rasayanjournal.com
http://www.rasayanjournal.co.in

SYNTHESIS, CHARACTERIZATION OF 2-[(Z)-{[6-AMINO-2-(4-CHLOROPHENYL) PYRIMIDIN-4-YL] IMINO} METHYL]-4-NITROPHENOL SCHIFF BASE WITH Mn (II), Co (II), Ni (II), Cu (II), Zn (II), Pt (II) FOR THEIR NANOPARTICLE AND ANTIBACTERIAL STUDIES

Manisha G. Kapade, Pooja P. Batawale, Uttara M. Raut and Manohar V. Lokhande✉

Department of Chemistry, Sathaye College (Autonomous), Mumbai, Maharashtra-400057, India
✉Corresponding Author: manohar2210@gmail.com

ABSTRACT

The green synthesis of novel 2-[(Z)-{[6-amino-2-(4-chlorophenyl) pyrimidin-4-yl] imino} methyl]-4-nitrophenol Schiff base complexes with Mn $^{2+}$, Co^{2+}, Ni^{2+}, Cu^{2+}, Zn^{2+} and Pt^{2+} was successfully synthesized. These synthesized materials underwent thorough characterization using various analytical and physicochemical techniques, including elemental analysis, molar conductivity, magnetic susceptibility, Fourier transform infrared (FTIR) spectroscopy, Electron spin resonance (ESR), Electronic spectra, Thermogravimetric analysis (TGA), Mass spectrometry, and X-ray powder diffraction. The results show that the Pt^{2+} and Ni^{2+} complexes exhibit octahedral geometry, while all other complexes adopt a square planar geometry. The ESR spectral data provided insights into their structures and the degree of covalency. Additionally, SEM and TEM studies showed that the synthesized nanoparticles have sizes ranging from 19-32 nm, with spherical granules. Furthermore, Schiff base and their metal ion complexes were tested for their anti-microbial activities.

Keywords: FTIR, MASS, SEM, TEM, Electronic Spectra, Magnetic Moments, And Thermal Analysis Studies.
RASĀYAN *J. Chem.*, Vol. 17, No.4, 2024

INTRODUCTION

Schiff bases, chemical compounds with the general formula $R_2C=NR'$, belong to a sub-class of imines. Depending on their structure, they can be either secondary ketoimines or secondary aldimines. [1,2] The general structure of a Schiff base is R─CH=N─R', where R and R' represent linear or cyclic alkyl and/or aryl groups that may be inversely substituted.[3] Recently, ligands coordination chemistry has gained attention for its relevance in analytical chemistry, electroplating, metallurgy, organic synthesis, Schiff bases find bids in various fields, including the dye industry, catalysis, fungicidal agents, and agrochemicals and photography.[4,5,6,7] Additionally, some Schiff bases exhibit remarkable antibacterial, antifungal, antimalarial, anti-inflammatory, antiviral, antipyretic, and anticancer activities. In this class of compounds, the >C=N- moiety plays a crucial role in biological activity. [8] These effects are attributed to the presence of an imine (>C=N-) linkage.[9] Conversely, Schiff base metal ion complexes have been discovered to have pharmacological and biological properties, such as anti-bacterial and anti-fungal activities.[10,11] The azomethine nitrogen, also known as the primary bonding point for the Schiff base, plays a crucial role. Additionally, the azomethine system, where the nitrogen atom is bonded via a double bond, serves as a coordination site for d-metal ions, facilitating back bonding through its π-orbitals. Consequently, the azomethine group with the nitrogen atom exhibits both σ-donor and π-acceptor functions, contributing to the high stability of metal complexes formed by Schiff bases.

These compounds can form stable chelate rings, such as quintet or hexavalent structures, with metal ions.[12-15] In this research paper, we are focused on the preparation of a novel Schiff-base of 2-[(Z)-{[6-amino-2-(4-chlorophenyl) pyrimidin-4-yl] imino} methyl]-4-nitrophenol and its novel metal ion complexes with Mn $^{2+}$, Co^{2+}, Ni^{2+}, Cu^{2+}, Zn^{2+} and Pt^{2+}. Several techniques like elemental analysis, FTIR, ESR, mass spectra, UV–visible, TGA, and magnetic studies, were used to characterize the produced

Schiff base and its complexes. TEM and XRD were used to determine the particle size and morphology of the complexes.

EXPERIMENTAL

All reagents used are of standard and laboratory quality. Prepare the solution using double distilled water. Characterization techniques used in infrared spectroscopy: Recorded using Perkins-Elmer Paragon-500 spectrophotometer and KBr particles. Electronic spectra: recorded on a Cintra-5 GBC UV-visible spectrophotometer. Magnetic susceptibility measurement: performed using Hg CO $(CNS)_4$ as a calibrator. TGA and DTA: Mettler recorded from 50°C to 900°C under atmospheric nitrogen in the Toledo Star System. X-ray powder diffraction: Recorded on a Joel-8030 dual goniometer X-ray powder diffractometer. Mass Spectrometry: Collection in Pharmaceutical Laboratories. Conductivity measurement: Performed using the Elico conductivity bridge. SEM (Scanning Electron Microscope): Used to examine nanoparticles. SEM sees electrons scattered from the surface. The machine used was a Quanta 200 ESEM. TEM (Transmission Electron Microscope): Also used for nanoparticle analysis. Elemental Analysis and Electron Spin Resonance: These analyses are done at IIT Mumbai. Finally, calculate the density of the complex in heavy toluene using a special vial.

Synthesis of Schiff Base

Add 1.68 g of 5-nitro-2-hydroxybenzaldehyde to a round bottom flask. 2-(4-chlorophenyl) pyrimidine-4,6-diamine (2.21g): 2.21g of 2-(4-chlorophenyl) pyrimidine-4,6 diamine was dissolved in 100 cm^3 of anhydrous (double distilled) alcohol. Mix the two solutions in a 1:1 molar ratio. The mixture is refluxed at 80° C on a hot magnetic plate for about 4 hours and a few drops of 1M acetic acid are used. After boiling, cool the reaction solution to 25°C, and pour the cooled solution into ice water. The resulting precipitate is separated. Filter the precipitate by using Whatman Paper No. 41, and finally wash with thoroughly with distilled water and absolute alcohol. The precipitate is dried at room temperature for 12 hours. The resulting products are called Schiff bases (Fig.-1).

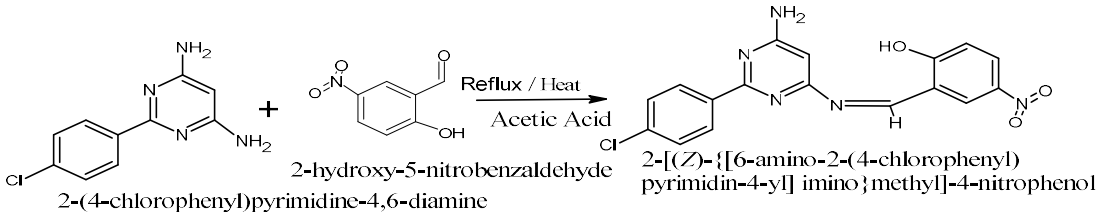

Fig.-1: Synthesis of Schiff Base

Synthesis of Complexes

Metal chlorides and nitrates Mn^{2+}, Co^{2+}, Ni^{2+}, Cu^{2+}, Zn^{2+}, and Pt^2 were dissolved in double-distilled water and the stock solutions of 0.1 M were prepared and a solution of Schiff's base (0.1 M) was prepared in absolute alcohol. The equimolar solutions of Schiff base (L) and metal ion (M) solution (both 0.1) were refluxed for two hours and thirty minutes with constant magnetic stirring on a hot plate. After complete refluxing, 2-3 drops of alcoholic ammonia (1:1) were added dropwise until a precipitate formed (Fig.2). This precipitate was then cooled, filtered, and washed with distilled water, followed by alcohol. Finally, the precipitate was dried in an oven at 60°C.

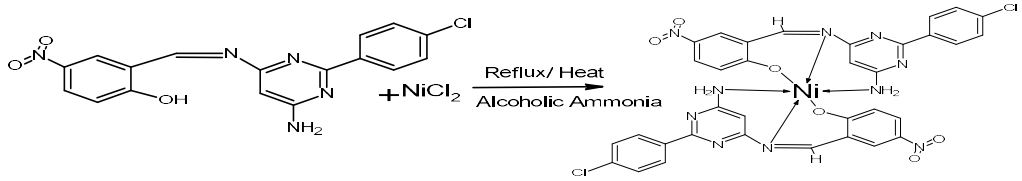

Fig.-2: Synthesis of Metal Ion Complexes with Schiff Base

Synthesis of Nanoparticles

The Schiff base and metal ion solution were mixed in equimolar concentration, first, it was refluxed for two hours then this solution was transferred in a test tube and centrifugated for three hours at 5000 RPM at room temperature. The fine powder of yellowish color crystal was obtained. These crystals are separated and stored in a closed container. These nanoparticles were given for Characterization.

RESULTS AND DISCUSSION

Analytical data for Schiff base complexes and metal ions are given in Table-1. These complexes have different colors, while the Zn (II) complex is colorless. Additionally, all complexes remained stable at room temperature. Most of these complexes are insoluble in organic solvents but are soluble in dimethyl sulfoxide (DMSO) and dimethylformamide (DMF). Decomposition occurs over a temperature range of 205Â°C to 230Â°C. It is important to note that the reported melting and decomposition temperatures were measured using the open capillary method and remain uncorrected. The molar conductivity value corresponds to the electrolytic properties of the composite. Conductivity is also observed in DMF at a molar solution concentration of 10^{-3}. Therefore, the resulting complex is essentially non-electrolyte.[16]

Table-1: Physical and Analytical Data (* Experimental Values)

Schiff base/ Complexes	% Yield	MP/ DPºC	C%	N%	M%	Ω^{-1} ol^{-1} cm^2	BM. μ_{eff}
$C_{17}H_{12}ClN_5O_3$	85	185-188	55.22 55.07*	18.94 18.82*	- -	-	-
$[Mn(C_{34}H_{24}Cl_2N_{10}O_6).2H_2O]$	70	215-218	51.40 51.24*	17.63 17.40*	6.92 6.78*	4.12	5.25
$[Co(C_{34}H_{24}Cl_2N_{10}O_6).2H_2O]$	68	212-215	51.14 50.98*	17.54 17.35*	7.38 7.22*	4.14	4.28
$[Ni(C_{34}H_{24}Cl_2N_{10}O_6).2H_2O]$	65	222-225	51.16 50.95*	17.55 17.38*	7.35 7.20*	5.18	3.22
$[Cu(C_{34}H_{24}Cl_2N_{10}O_6).2H_2O]$	64	220-222	50.85 50.71*	17.44 17.28*	7.91 7.73*	5.12	1.75
$[Zn(C_{34}H_{24}Cl_2N_{10}O_6).2H_2O]$	66	214-217	50.73 50.59*	17.40 17.20*	8.13 7.98*	4.75	Dimag
$[Pt(C_{34}H_{24}Cl_2N_{10}O_6).2H_2O]$	58	208-211	43.69 43.51*	14.99 14.78*	20.87 20.68*	4.71	-

Magnetic Properties

The revised magnetic moment (μ_{eff}) units are listed (Table-1). Some complexes are paramagnetic magnetic except the Zn (II) complex is diamagnetic. [17,18] These complexes indicate that they slightly participate in the 3d electrons in bond formation.

IR Spectra of Schiff Base and Complexes

Infrared spectroscopy is a helpful technique for determining and verifying the structure of organic molecules. It involves analyzing band frequencies between 4000- 300 cm^{-1} **(**wavelength). Specifically, this technique focuses on infrared and its application. The important infrared frequencies of both ligands and complexes, along with their tasks are given below. Here are the key observations from comparing the IR spectra of the ligand and their metal ion complexes (Fig.-3 and 4).

The Similarity in Spectra

The IR spectra of the Schiff base closely look like those of the metal complexes at 485-665 cm^{-1}.

Distinctive Absence

Ligands exhibit the nonappearance of bands around 1627 cm^{-1} 3150 cm^{-1} and 3391 cm^{-1}. These missing bands correspond to the characteristic stretching vibrations of the azomethine group (>C=N-), amino (-NH_2), and a hydroxyl group (-OH) in the respecting starting material.[19,20,21]

New Bands in Chelates

In chelates, new bands appear at 1652 cm^{-1} owing to the azomethine linkage (>C=N-). These observations strongly support the development of the Schiff base.

Azomethine Nitrogen Coordination

The changing in the bands of the azomethine group to the higher frequency sideways (in between 05-25 cm^{-1}) provides further evidence of the participation of azomethine nitrogen in coordination through the metal ions.

Amino Group Coordination the individual bands associated with the amino group seem at the lower frequency side (approximately 15-40 cm^{-1}) in the IR spectra of the metal complexes. This recommends that coordination of the ligand occurs through the nitrogen atoms of the amino group to the metal atom at 3186-3205 cm^{-1}.

Hydroxyl Stretching Vibration and Far IR Region Bands

A broad band of about 3391cm^{-1} can be seen in the spectrum of the ligand due to the hydroxyl (-OH) stretching vibration. However, this band disappears in the spectrum of the complex. A new band appears at 1186-1257 cm^{-1} due to the (>C-O) frequency. This change supports the idea that the hydroxyl group plays a role in chelation and deprotonation. Metal-nitrogen and metal-oxygen bands at 480-490 cm^{-1} and 660-670 cm^{-1} for complexes.[24,25] Then, the -NH_2 group of the nitrogen, the azomethine of the nitrogen, and the deprotonated oxygen of the hydroxyl moiety participate in chelation.

Coordinatized Water Molecules

In the higher region bands were observed at 3410-3425 cm-1 and 3530-3540 cm^{-1} parallel to the presence of two coordinated water molecules in the coordination sphere.

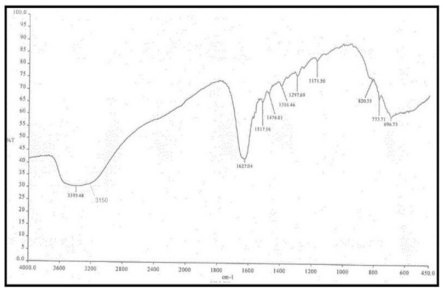

Fig.-3: FTIR of Schiff Base

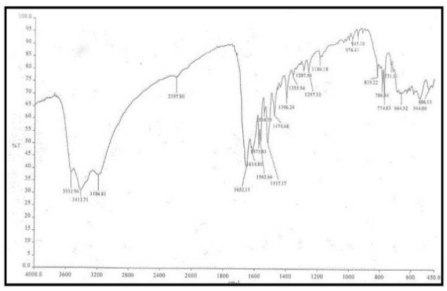

Fig.-4: FTIR of [Ni- Complex]

SEM TEM and EDX Image of Cu NPs

The SEM micrograph of 2-[(Z)-{[6-amino-2-(4-chlorophenyl) pyrimidin-4-yl] imino} methyl]-4-nitrophenol with copper nanoparticles (CuNPs) is shown in the below figure. The surface appears porous, with some inclusions. Notably, copper nanoparticles exhibit a homogeneous distribution on the matrix surface. A similar appearance is observed in the figure for the Schiff base with copper nanoparticles, albeit with a larger particle size**,** as elucidated by TEM. This increase in size may be attributed to the presence of 2-[(Z)-{[6-amino-2-(4-chlorophenyl) pyrimidin-4-yl] imino} methyl]-4-nitrophenol within the investigated nanocomposite. The surface morphology of the Schiff base reveals a rough appearance, while the CuNPs are evenly distributed throughout the entire matrix, as illustrated in the figure. Fewer cavities are observed on the surface of Schiff bases, along with some roughness (as shown in the figure). This phenomenon could be attributed to 2-[(Z)-{[6-amino-2-(4-chlorophenyl) pyrimidin-4-yl] imino} methyl]-4-nitrophenol, which contributes to greater uniformity and consistency in the structure of the Schiff base during the development of spherically formed copper nanoparticles.[26]

Moving on to Transmission Electron Microscopy (TEM), the figure illustrates the TEM micrograph of the nanocomposite loaded with copper nanoparticles (CuNPs). The distribution of CuNPs inside the matrix shows acceptable dispersion, with particle sizes ranging from 19-32 nm (Fig.-5,6, and 7).

Electronic Spectra of Complexes

The electronic spectra play a vital role in calculations, determining spectral parameters, and other structural investigations. These spectra allow us to assign various parameters related to covalency, bonding, and more for metal chelates based on their locations and the number of d–d transition peaks. The spectra of chelates were recorded at (0.0001M) concentration for individually complex in DMF in the range of 300−900 nm. However, it's important to note that the spectra for Mn^{2+} and Co^{2+} in 0.0001M solutions were taken in the visible region.

Manganese (II) Complex

The spectrum of the complex [Mn ($C_{34}H_{24}Cl_2N_{10}O_6$) .$2H_2O$] shows three bands at 24,096 cm^{-1} (415 nm), assigned to $^4T_{1g} \rightarrow {}^6A_{1g}$ transition, 17094 cm^{-1} (585 nm), assigned to $^4T_{2g}(G) \rightarrow {}^6A_{1g}$ transition, 12,853 cm^{-1} (778 nm), assigned to $^4T_{1g}(D) \rightarrow {}^6A_{1g}$ transition (Fig.8). These transitions suggest an octahedral geometry.[27,28,29]

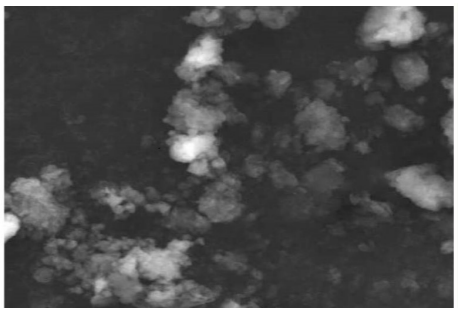

Fig.-5: SEM Image of CuNPs

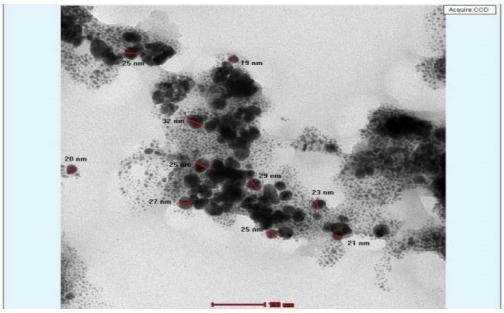

Fig.-6: TEM Image of CuNPs

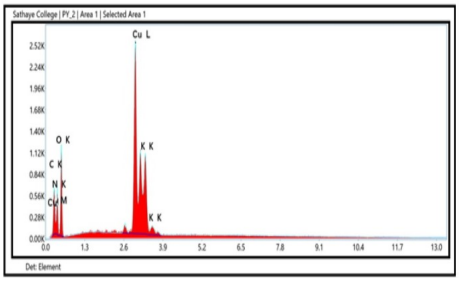

Fig.-7: EDX of CuNPs

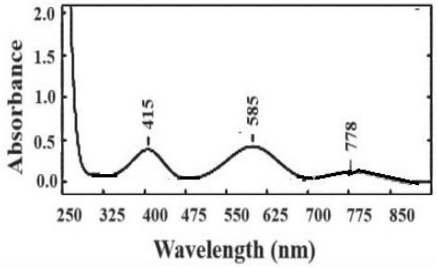

Fig.-8: UV-Visible of [Mn- Complex]

Cobalt (II) Complex

The electronic spectrum of the complex [Co ($C_{34}H_{24}Cl_2N_{10}O_6$) .$2H_2O$] generally shows three absorption bands at 23,225 cm^{-1} (430 nm), assigned to $^4T_{1g} \rightarrow {}^4T_{2g}(F)$ transition, 16722 cm^{-1} (598 nm), assigned to $^4T_{1g} \rightarrow {}^4A_{2g}(F)$ transition, 12468 cm^{-1} (802 nm), assigned to $^4T_{1g} \rightarrow {}^4T_g(P)$ transition. These transitions indicate octahedral geometry around the Co (II) ion (Fig.-9). These electronic spectra provide valuable insights into the coordination environment and structural properties of these metal complexes.[30] The size of the red band function (β) [31], correlation coefficient ($b_{1/2}$) [32], and Sinha parameter (% β) were calculated.

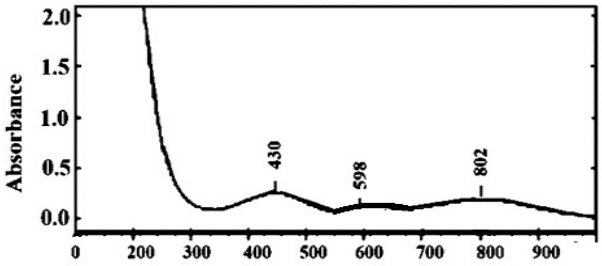

Fig.-9: UV-Visible of [Co-Complex]

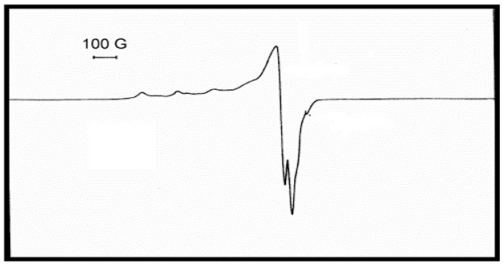

Fig.-10: ESR of Copper Complex

Table-2: Electronic Spectral Parameters

Complexes	Bands (cm^{-1})	Assignments	Parameters
[Mn ($C_{34}H_{24}Cl_2N_{10}O_6$).$2H_2O$]	24,096 17094 12,853	$^4T_{1g} \rightarrow {}^6A_{1g}$ $^4T_{2g}(G) \rightarrow {}^6A_{1g}$ $^4T_{1g}(D) \rightarrow {}^6A_{1g}$	β = 0.9748 δ = 1.2895 $b^{1/2}$ =0.0793 η = 0.0128
[Co ($C_{34}H_{24}Cl_2N_{10}O_6$) .$2H_2O$]	23,225 16722 12468	$^4T_{1g} \rightarrow {}^4T_{2g}(F)$ $^4T_{1g} \rightarrow {}^4A_{2g}(F)$ $^4T_{1g} \rightarrow {}^4T_g(P)$	β = 0.9712 δ = 1.5032 $b^{1/2}$ =0.0848 η = 0.0148

Electron Spin Resonance

ESR Spectra of [Copper complex] were recorded at room temperature [33]. Four similar solutions exist for g‖ (2.3124) and g⊥ (2.1123) in the lower region. For the Cu^{2+} complex, the observed difference between g‖ (2.3124) > g (2.1123) > g_e (2.0095) indicates that, the unpaired electrons are locked in the dx^2-y^2 orbital of Cu ions [34,35]. This supports that the value of 'G' interaction can be estimated by the expression: G = (g‖2.0095) /(g⊥2.0095)/(g−2.0095)→2.0095), the alignment of finite axes is the same or only slightly skewed. Conversely, if (G < 4.0), there is a significant and negative correlation change. The G value of 3-82 indicates negligible Cu-Cu exchange contact in the chelate. The spin-orbit coupling constant, d denoted (lambda) (value -15589 cm^{-1}), is calculated using the following relationship: g_{av} = 1/3 (g- + 2 g-') and g_{av} = 2(1 → 2Î/ 10Dq). This value is smaller than free Cu(II) ions (−12012 cm^{-1}), supporting the complex's covalent nature of the M-L band. The g value of the Cu^{2+} complex is less than 2.48, indicating the covalent character of the M-L bond.

Mass Spectra of Schiff Base and Complex

The spectrum of the complexes was recorded at 25 °C. Ligand [L] shows a molecular ion peak at m/z 369.1, equal to the peak [L+H] calculated from m/z value 369 (Fig.-11). The mass spectrum of the Ni^{2+} complex shows a molecular ion peak at m/z = 832.231; this corresponds to the molecular weight of the compound. In comparison, the Ni^{2+} complex has [M+1] of m/z = 832.231 and dis plays both [M+1] and [M+2] modes. Additionally, the molecular ion peak at m/z 338 corresponds to the carbon ion present in the metal complex. These peaks provide support for the structure of the complex and confirm that its stoichiometry is of the ML_2 type [36].

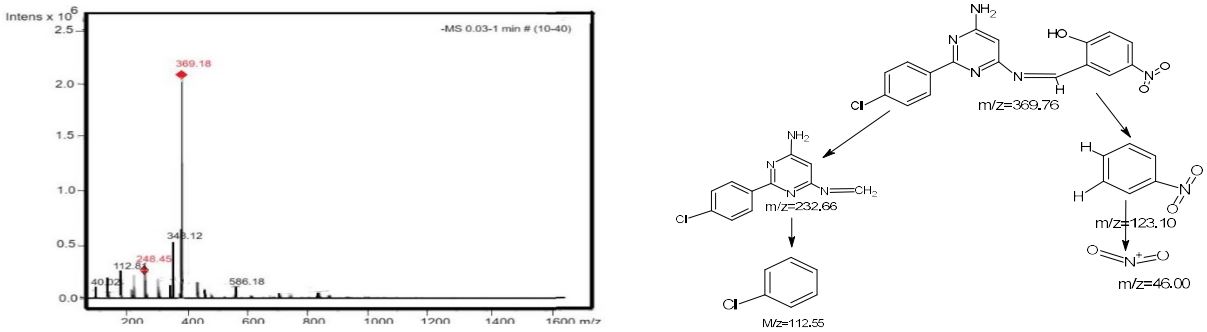

Fig.-11: Mass spectra of Schiff Base

Thermal analysis of Schiff base Complex: Complex lose their molecular weight due to exothermic and endothermic reactions.[36] The complex is thermally stable at Room temperature and decomposes in Four stages.

$$[Pt(C_{34}H_{24}Cl_2N_{10}O_6).2H_2O] \xrightarrow{50\text{-}200°C} [Pt(C_{28}H_{20}Cl_2N_8O_6)] \xrightarrow{200\text{-}300°C}$$

$$[Pt(C_{24}H_{12}ClN_6O_6)] \xrightarrow{310\text{-}415\ °C} [Pt(C_{20}H_5ClN_5O_6)] \xrightarrow{415\text{-}940°C} PtO$$

Complex	Temp range °C	Calculated Value %	Expt. values %	Possible leaving groups
[$Pt(C_{34}H_{24}Cl_2N_{10}O_6)$.$2H_2O$	50-200	11.12	11.08	$C_6H_4N_2.2H_2O$
	200-300	23.05	22.00	$C_4H_8N_2Cl$
	300-470	30.22	30.18	C_4H_5N
	470-800	35.12	35.09	PtO

X-ray Powder Diffraction Complex

Record and scan the X-ray diffraction pattern of [$Cu(C_{34}H_{24}Cl_2N_{10}O_6).2H_2O$] information about the diffractogram describes the 2θ value, the equilibrium constant, and the relative difference (d value) of each peak.[37]

The indexing process also yields the Miller Performance index (hkl), unit cell parameters, volume, and density of the composite; these are calculated and tabulated in (Fig.-13) and (Table-3).

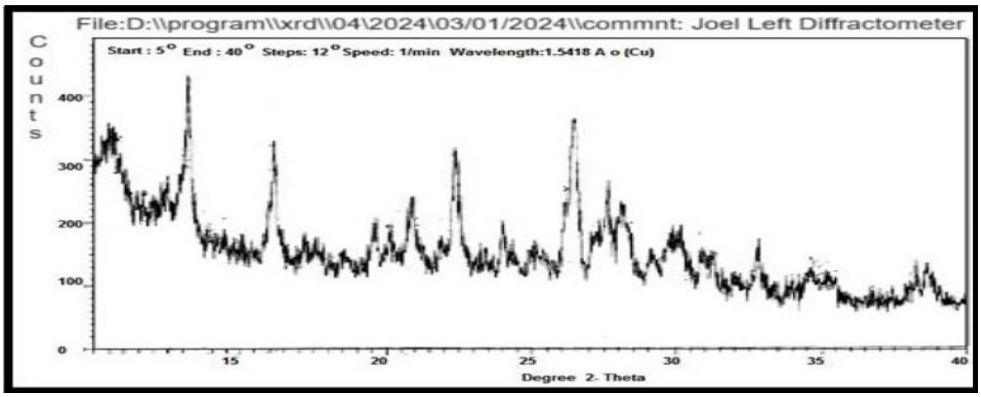

Fig.-13. X-RD Powder of [Cu-Complex]

Table-3: X-RD of [Cu- Complex]

System: Monoclinic-P Lambda: 1.5418 Å E=51.39

A=85.18 Å a=8.8912 Å beta=111.11.D

B=19.24 Å b=17.5145 Å V=2243.36 Å

C= 65.87 Å c= 10.0428 Å D=1.9452 g /cm^{-3}

No	d-Spacing A °		Indices			$Sin^2\theta$		2θ Degree			I/I_O
	Obs.	Calc.	h	k	l	Obs.	Calc.	Obs.	Calc.	Diff	
1	8.3782	8.3782	1	0	0	84.5	84.5	10.55	10.55	0.00	78
2	8.2997	8.2997	0	1	1	86.1	86.1	10.65	10.65	0.00	100
3	7.7081	7.7081	1	0	1	99.9	99.9	11.47	11.47	0.00	35
4	7.5571	7.5571	1	1	0	103.9	103.9	11.70	11.70	0.00	38
5	7.0304	7.0521	1	1	1	120.0	119.2	11.58	11.54	0.04	38
6	6.5149	6.4139	0	2	1	139.8	144.2	13.58	13.79	-0.21	27
7	6.1035	6.0521	1	2	0	159.3	162.0	14.50	14.62	-0.12	41
8	5.8431	5.8347	0	3	0	173.8	174.3	15.15	15.17	-0.02	68
9	5.4700	5.4099	1	0	1	198.3	202.7	16.19	16.37	-0.18	45
10	5.1451	5.1687	1	1	1	224.1	222.1	17.22	17.14	0.79	49
11	4.3815	4.3761	0	4	0	309.0	309.8	20.25	20.28	-0.02	43
12	3.4928	3.5008	0	5	0	486.1	484.1	25.48	25.42	0.06	78
13	3.3971	3.4023	1	4	1	514.1	512.5	26.21	26.17	0.04	48
14	3.2781	3.2818	0	5	1	552.1	550.9	27.18	27.15	0.03	65
15	3.1324	3.1423	0	0	3	604.7	600.9	28.47	28.38	0.09	49
16	3.0619	3.0678	2	0	3	632.8	630.4	29.14	29.08	0.05	61
17	2.9061	2.9002	1	3	3	702.5	705.4	30.74	30.80	-0.06	58
18	2.8465	2.8454	1	5	2	732.2	732.8	31.40	31.41	-0.01	54
19	2.7477	2.8454	2	5	1	785.9	786.1	32.56	32.56	-0.01	38
20	2.6619	2.6606	3	2	0	837.3	838.2	33.64	33.66	-0.02	31
21	2.6210	2.6230	1	1	3	863.6	859.1	34.18	34.09	0.09	39
22	2.5279	2.5190	3	3	0	928.4	935.0	35.48	35.61	-0.12	37
23	2.4415	2.4420	2	0	4	995.3	994.9	36.78	36.77	0.00	24

Anti-Bacterial Activity of Schiff Base and Complexes

Ligands and their complexes prepared using standard streptomycin and agar as media were evaluated by the positive diffusion method against the following bacteria.[38,39] The Ligand 2-[(Z)-{[6-amino-2-(4-chlorophenyl) pyrimidin-4-yl] imino} methyl]-4-nitrophenol (**C_{17} H_{12} ClN_5O_3**), was showing the activity against all micro-organisms with its [Mn-Complex] and [Ni-Complex] complexes show more reasonable but enhanced activity. However, the [Cu-Complex] and [Pt-Complex] complexes are more dynamic against both bacterial strains.

Table-4: Anti-Bacterial Activity of Schiff Base and Complexes

Schiff base/ Complexes	Gram-negative Bacteria		Gram Positive bacteria	
	Salmonella	E. Coli	Actinomyces	B. Subtilis
$C_{17}H_{12}ClN_5O_3$	14	16	10	12
$[Mn(C_{17}H_{12}ClN_5O_3)_2.2H_2O]$	17	18	19	21
$[Ni(C_{17}H_{12}ClN_5O_3)_2.2H_2O]$	15	18	20	17
$[Cu(C_{17}H_{12}ClN_5O_3)_2.2H_2O]$	19	23	21	24
$[Pt(C_{17}H_{12}ClN_5O_3)_2.2H_2O]$	20	22	23	25

CONCLUSION

The Schiff base 2-[(Z)-{[6-amino-2-(4-chlorophenyl) pyrimidin-4-yl] imino} methyl]-4-nitrophenol was prepared and characterized using various instrumental techniques. Metal ion complexes of Mn^{2+}, Co^{2+}, Ni^{2+}, Cu^{2+}, Zn^{2+}, and Pt^{2+} were synthesized. The anti-microbial activity of both the ligand and its complexes was studied. Electronic spectra analysis indicated that the complexes exhibit covalent behavior, while XRD studies revealed that the complexes have a monoclinic crystal structure with a density of 1.9425 g/cm³. The nanoparticles (NPs) formed from these complexes exhibit a spherical shape, with particle sizes ranging from 19 to 32 nm and a mean size of 25 nm. FTIR spectra analysis suggests the involvement of azomethine and hydroxyl moieties in complex formation. Finally, the biosynthesized CuNPs are expected to have remarkable applications.

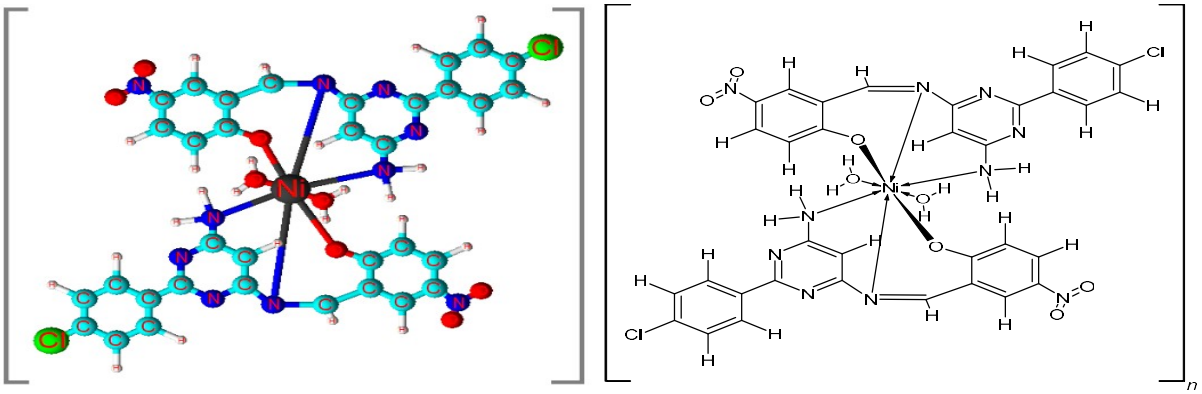

Fig.-14: Proposed Structure of Complex

ACKNOWLEDGMENTS

All authors thank to Principal, HOD, Chemistry of Sathaye College, Mumbai. We are also thankful for providing SEM, TEM, and EDX facility ICON Labs, Mumbai. ESR -IIT MUMBAI, FTIR, and all other instrumental facilities provided by the University of Mumbai.

CONFLICT OF INTERESTS

The authors declare that there is no conflict of interest, financial or otherwise.

AUTHOR CONTRIBUTIONS

All the authors contributed significantly to this manuscript, participated in reviewing/editing, and approved the final draft for publication. The research profile of the authors can be verified from their ORCID IDs, given below:

Manohar V. Lokhande https://orcid.org/0000-0002-7521-1262
Manisha G. Kapade https://orcid.org/0009-0006-1227-2988
Pooja P. Batawale https://orcid.org/0009-0002-7188-8409
Uttara M. Dalvi https://orcid.org/0009-0008-4417-6151

REFERENCES

1. V. K. Rao, S. S. Reddy, B. S. Krishna, K. R. Mohan Naidu, C. N. Raju and S.K. Ghosh, *Green Chemistry Letters and Review,* **3,** 217 (2010), https://doi.org/10.1080/17518251003716550
2. F.A. Carey, 2003, *Organic Chemistry*, 5th ed. MacGraw-Hill, New York, pp. 724.
3. N. R. Bader, *Rasayan Journal of Chemistry*, **3**(4), 660 (2010).
4. P.A. Vigato and S. Tamburini, *Coordination Chemistry Review,* **248**, 1717(2004), https://doi.org/10.1016/j.cct.2003.09.003
5. L.H. Abdel-Rahman, A.M. Abu-Dief, M.R. Shehata, F.M. Alam and A.A. Hassan Abdel-Mawgoud, *Applied Organometallic Chemistry,* **33,** e4699(2019), https://doi.org/10.1002/aoc.4699
6. M.S. More, P.G. Joshi, Y.K. Mishra and P.K. Khanna, *Materials Todays Chemistry,* **14**, 100195 (2019), https://doi.org/10.1016/j.mtchem.2019.100195
7. M. J. Gemi, C. Biles, B.J.Keiser, S.M.Poppe, S.M.Swaney, W.G.Tarapley, D.L.Romeso and Yage, *Journal of Medicinal Chemistry,* **43,**1034, (2000), https://doi.org/10.1021/jm990383f
8. K. Sirumalar, M. Paul Johnpeter, R. Manikandan, A. P. Mary Sri Archana and A. Paulraj, *Rasayan Journal of Chemistry,* **14**, 1316 (2021), https://doi.org/10.31788/RJC.2021.1426283
9. S.M. Wilkinson, T.M. Sheedy and E. J. New, *Journal of Chemical Education,* **93**, 351(2016), https://doi.org/10.1021/acs.jchemed.5b00555
10. E.Yousif, A.Majeed, K.Al-Sammarrae, N. Salih, J. Salimon and B.Abdullah, *Arabian Journal of Chemistry,* **10**, S1639 (2017), https://doi.org/10.1016/j.arabjc.2013.06.006
11. T.Vadivel and M.Dhamodaran, *International Journal of Biological and Macromolecules,* **90**, 44 (2016), https://doi.org/10.1016/j.ijbiomac.2015.11.008
12. O.Catanescu, M. Grigoras, G. Colotin, A. Dobreanu, N. Hurduc and C. Simionescu, *European Polymer Journal,* **37,** 2213 (2001), https://doi.org/10.1016/S0014-3057(01)00119-7
13. M.B. Smith and J. March, 2007, Advanced Organic Chemistry, NY, USA, Wiley.
14. N. Ancin, S. Ide, S. G. Ozta, M. Tuzun, *Journal of Molecular Structure,* **606,** 45(2002), https://doi.org/10.1016/S0022-2860(01)00812-2
15. L.H. Abdel-Rahman, A.M. Abu-Dief, R.M. El-Khatib and S.M. Abdel-Fatah, *Bioorganic Chemistry,* **69**, 140(2016), https://doi.org/10.1016/j.bioorg.2016.10.009
16. N. Raman, S. Sobha and L. Mitu, *Journal of Saudi Chemical Society*, **17**, 151(2013), https://doi.org/10.1016/j.jscs.2011.03.003
17. N. S. Hosmane, 2017, Advanced Inorganic Chemistry, Academic Press, pp. 89.
18. F.A. Cotton, 2007, Advanced Inorganic Chemistry, 6th Edn. John Wiley and Sons, pp.633.
19. S.Arulmurugan, H.P. Kavitha and B.R. Venkatraman, *Rasayan Journal of Chemistry,***3(3)**, 385(2010).
20. M. Bashir and A.A.Dar, I. Yousuf, *ACS Omega,* **8**, 3026(2023), https://doi.org/10.1021/acsomega.2c05927
21. J. Sebastian, M. K. Muraleedharan Nair and S. Sasi1, *Rasayan Journal of Chemistry,***15(2***),* 1202(2022), https://doi.org/10.31788/RJC.2022.1526789
22. K. George and M.V. Lokhande, *International Journal of Pharmaceutical Science and Research,* **8(8)**,3413 (2017), https://doi.org/10.13040/IJPSR.0975-8232.8(8).3413-20
23. M.V. Lokhande and M.R. Choudhary , *International Journal of Pharmaceutical Science and Research,* **5(5),**1757 (2014), https://doi.org/10.13040/IJPSR.0975-8232.5(5).1757-66
24. Y. Satyawana, R. Meena, R. V. Singh and N. Fahmi., *Rasayan Journal of Chemistry*, **12(4)**, 2328, (2019), https://doi.org/10.31788/RJC.2019.1245459
25. K. Nakamoto, Infrared and Raman Spectra of Inorganic and Coordination Compounds, Part B, Wiley, p.221,228(1997).
26. K. Singh, B. Kumari and A. Sharma, *Rasayan Journal of Chemistry*,**14(1)**, 29(2021), https://doi.org/10.31788/RJC.2021.1416108
27. H. Huang, Q. Yuan and X. Yang, *Colloids and Surfaces B: Biointerfaces,* **39**, 31(2004), https://doi.org/10.1016/j.colsurfb.2004.08.014
28. F. A. Cotton, G. Wilkinson, C. A. Murillo, 1999, Advanced Inorganic Chem, 6th edn, NY, pp.455.
29. G. L. Miessler and T. A. Donald, Inorganic Chemistry, Prentice-Hall, 2nd edn., pp.377(1999).

30. W. Al Zoubi, and Y. G Ko, *Journal of Organometallic Chemistry,* **822**, 173(2016), https://doi.org/10.1016/j.jorganchem.2016.08.023
31. R. Vindhya, T. M. Sharanakumar, V. Kumar, A. Kalalbandi1, K. N. Shashiraj, K. M. Nagarsha, H. M. Suresh Babu, and Suresh, *Rasayan Journal of Chemistry*, **17(3)**, 945(2024), https://doi.org/10.31788/RJC.2024.1738886
32. G. Farooq and M.V. Lokhande, *IOSR Journal of Applied Chemistry,* **7**,21(2014), https://doi.org/10.9790/5736-07212732
33. P.Masarova, V. Kuchtanin and M.Mazur, *Transitional Metal Chemistry,* **43**,507 (2018), https://doi.org/10.1007/s11243-018-0236-2
34. G. Sciortino, M. Jean-Didier, I. Fabian, N. Lihi and E. Garribba, *Journal of Inorganic Biochemistry,* **204**, 110953 (2020), https://doi.org/10.1016/j.jinorgbio.2019.110953
35. N. Tereba, T. Muziol, R. Podgajny and G. Wrzeszcz, *Crystals***,** **9**,637(2019), https://doi.org/10.3390/cryst9120637
36. M. Shakir, A. Abbasi, M. Faraz and A.Sherwani, *Journal of Molecular Structures,* **1102**,108 (2015), https://doi.org/10.1016/j.molstruc.2015.08.061
37. M. Baskar and A. Patania, *Journal of Biophysical Chemistry,* **11,**51(2020), https://doi.org/10.4236/jbpc.2020.114005
38. J.H. Grosset and T. Singer, Streptomycin, Brenner's Encyclopaedia of Genetics, 2nd Edn., pp. 568(2014).
39. R.J. Wallace Jr, J.V. Philley and D.E. Griffith, Antimycobacterial Agents, Mandell, Douglas, and Bennett's Principles and Practice of Infectious Diseases, 8th Edn., pp.463 (2015).

[RJC-8925/2024]